Preprints of the 21st IFAC World Congress (Virtual)
Berlin, Germany, July 12-17, 2020

Stable Force Reconstruction from Acceleration Measurements - Theory and Experiment

Roland Falkensteiner * **Richard Seeber** *, ** **Martin Horn** *, **
Robert Tafner *

* *Institute of Automation and Control, Graz University of Technology, 8010 Graz, Austria (e-mail: roland.falkensteiner@tugraz.at)*
** *Christian Doppler Laboratory for Model Based Control of Complex Test Bed Systems, Institute of Automation and Control, Graz University of Technology, Graz, Austria*

Abstract: This paper presents an unknown input observer for the estimation of external forces acting on mechanical systems from only acceleration measurements. To circumvent arising stability issues, a classical unknown input observer extended with an additional filter is proposed. The influence of the design parameter of the filter is analyzed. A guideline for the parameter tuning depending on predefined estimation goals is given. In contrast to existing methods, no prior knowledge about the unknown acting force is assumed in the design process. The performance of the presented concept is compared to a state-of-the-art approach in both simulation studies and on a experimental test setup.

Keywords: observer design, unknown input observer, force reconstruction, strong observability and detectability

1. INTRODUCTION

External forces acting on mechanical structures like buildings, machinery or vehicles are of great interest, for example in fault detection, structural analysis, or system monitoring. However, direct force measurement is often impossible and the forces have to be reconstructed via measurements of the structure's movements in combination with an a priori known system model. These movements can be determined by different sensor types. The most common ones are acceleration sensors due to their simple mounting, high dynamic range and independence of a reference point. This paper focuses on systems where acceleration sensors are employed exclusively.

Force reconstruction from acceleration measurements is an ill-posed inverse problem. An overview of regularization methods for the solution of inverse problems is given in Sanchez and Benaroya (2014). However, all regularization methods are still sensitive with respect to measurement noise. An alternative approach is to find a mathematical system description with the external force as an unknown input and to use observer concepts for force reconstruction. These observers can either use deterministic models, as in Klinkov (2011), or stochastic models, as the Kalman filter concepts presented in Lourens et al. (2012) and Eftekhar Azam et al. (2015). Both approaches encounter stability issues for systems with acceleration-only measurement as described in Maes et al. (2015). An augmented Kalman filter (AKF) with so-called dummy measurements for circumventing the stability issues is proposed in Naets et al. (2015). A drawback of this idea is that a realistic estimate of the magnitude for the structure's movements is necessary for the tuning of the AKF, but the movement depends on the amplitude and frequency of the excitation force.

In the present paper a classical unknown input observer (UIO) augmented with an additional filter for stabilization is designed. In contrast to the AKF approach, *no* prior knowledge of the excitation force amplitude nor frequency is assumed in the design process. A filter parameter is used for observer tuning and its influence on the observer performance is analyzed. A guideline for choosing an appropriate parameter depending on requirements for signal frequency range and noise amplification is given.

2. SYSTEM MODELING

The motion of a linear mechanical system with proportional damping discretized in space can be described by

$$\mathbf{M}\ddot{\mathbf{u}} + \mathbf{C}\dot{\mathbf{u}} + \mathbf{K}\mathbf{u} = \mathbf{S}_\mathrm{d}\mathbf{d} \tag{1}$$

$$\mathbf{y} = \mathbf{S}_\mathrm{a}\ddot{\mathbf{u}}, \tag{2}$$

where $\mathbf{u} \in \mathbb{R}^k$ is the vector of displacements of all considered degrees of freedom (DOFs), $\mathbf{M}$, $\mathbf{C}$ and $\mathbf{K} \in \mathbb{R}^{k\times k}$ are the mass, the damping and the stiffness matrices, respectively, $\mathbf{d} \in \mathbb{R}^q$ is the vector of excitation forces, and $\mathbf{S}_\mathrm{d} \in \mathbb{R}^{k\times q}$ is a selection matrix for the DOF, where excitation forces act. In this paper all considered outputs of the system are acceleration sensors $\mathbf{y}$ where $\mathbf{S}_\mathrm{a} \in \mathbb{R}^{p\times k}$ is a selection matrix for the DOFs at which the acceleration

⋆ The financial support by the Christian Doppler Research Association, the Austrian Federal Ministry for Digital and Economic Affairs and the National Foundation for Research, Technology and Development is gratefully acknowledged.

is measured. It is common to transform system (1) into modal coordinates due to easier experimental parameter identification and potential mode reduction.

2.1 Modal Model

Caughey (1960) describes a method for transforming (1) into a modal model by solving the generalized eigenvalue problem for the undamped system

$$\mathbf{K}\mathbf{\Phi} = \mathbf{M}\mathbf{\Phi}\mathbf{\Omega}^2 \tag{3}$$

where the eigenvectors are collected in the matrix $\mathbf{\Phi} \in \mathbb{R}^{k\times k}$ and $\mathbf{\Omega} = \operatorname{diag}(\omega_{0,1}, \omega_{0,2}, \ldots, \omega_{0,k})$ is a diagonal matrix containing the resonance frequencies $\omega_{0,j}$, $(j = 1, \ldots, k)$, of the system. The additional design freedom in eigenvector calculation is used for a scaling, such that the mass matrix is normalized according to

$$\mathbf{\Phi}^{\mathrm{T}}\mathbf{M}\mathbf{\Phi} = \mathbf{I}. \tag{4}$$

The matrix $\mathbf{\Phi}$ can be used for a transformation

$$\mathbf{z} = \mathbf{\Phi}^{-1}\mathbf{u} \tag{5}$$

from displacement into modal coordinates $\mathbf{z} \in \mathbb{R}^k$. Applying the transformation to (1), results in system description

$$\ddot{\mathbf{z}} + \mathbf{\Gamma}\dot{\mathbf{z}} + \mathbf{\Omega}^2\mathbf{z} = \mathbf{\Phi}^{\mathrm{T}}\mathbf{S}_{\mathrm{d}}\mathbf{d} \tag{6}$$

where $\mathbf{\Gamma} = \operatorname{diag}(\gamma_1, \gamma_2, \ldots, \gamma_k)$ is a diagonal matrix containing the modal damping ratios γ_j, $(j = 1, \ldots, k)$. The transformed output reads as

$$\mathbf{y} = \mathbf{S}_{\mathrm{a}}\mathbf{\Phi}\ddot{\mathbf{z}} = -\mathbf{S}_{\mathrm{a}}\mathbf{\Phi}\mathbf{\Omega}^2\mathbf{z} - \mathbf{S}_{\mathrm{a}}\mathbf{\Phi}\mathbf{\Gamma}\dot{\mathbf{z}} + \mathbf{S}_{\mathrm{a}}\mathbf{\Phi}\mathbf{\Phi}^{\mathrm{T}}\mathbf{S}_{\mathrm{d}}\mathbf{d}. \tag{7}$$

In this paper the SISO case ($p = q = 1$) is considered and only one column of $\mathbf{\Phi}$ is selected through $\mathbf{S}_{\mathrm{d}}$ and $\mathbf{S}_{\mathrm{a}}$. Therefore the results of the matrix products

$$\boldsymbol{\varphi}_{\mathrm{d}} = \mathbf{\Phi}^{\mathrm{T}}\mathbf{S}_{\mathrm{d}} = [\varphi_{\mathrm{d}1}\ \varphi_{\mathrm{d}2}\ \ldots\ \varphi_{\mathrm{d}k}]^{\mathrm{T}} \tag{8}$$

$$\boldsymbol{\varphi}_{\mathrm{y}}^{\mathrm{T}} = \mathbf{S}_{\mathrm{a}}\mathbf{\Phi} = [\varphi_{\mathrm{y}1}\ \varphi_{\mathrm{y}2}\ \ldots\ \varphi_{\mathrm{y}k}] \tag{9}$$

reduce to vectors $\boldsymbol{\varphi}_{\mathrm{d}}$ and $\boldsymbol{\varphi}_{\mathrm{y}}^{\mathrm{T}}$ for input and output, respectively, with entries for every mode k. Substituting (8) and (9) into (6) and (7) gives

$$\ddot{\mathbf{z}} + \mathbf{\Gamma}\dot{\mathbf{z}} + \mathbf{\Omega}^2\mathbf{z} = \boldsymbol{\varphi}_{\mathrm{d}}d \tag{10}$$

$$-\boldsymbol{\varphi}_{\mathrm{y}}^{\mathrm{T}}\mathbf{\Omega}^2\mathbf{z} - \boldsymbol{\varphi}_{\mathrm{y}}^{\mathrm{T}}\mathbf{\Gamma}\dot{\mathbf{z}} + \boldsymbol{\varphi}_{\mathrm{y}}^{\mathrm{T}}\boldsymbol{\varphi}_{\mathrm{d}}d = y. \tag{11}$$

By introducing the state vector $\mathbf{x} \in \mathbb{R}^{2k}$

$$\mathbf{x} = \left[\mathbf{z}^{\mathrm{T}}\ \dot{\mathbf{z}}^{\mathrm{T}}\right]^{\mathrm{T}} \tag{12}$$

the modal equation of motion (10) and the output equation (11) can be rewritten as a linear state space model

$$\Sigma: \begin{aligned} \dot{\mathbf{x}} &= \mathbf{A}\mathbf{x} + \mathbf{e}d \\ y &= \mathbf{c}^{\mathrm{T}}\mathbf{x} + fd \end{aligned} \tag{13}$$

with the system matrices $\mathbf{A} \in \mathbb{R}^{2k\times 2k}$, $\mathbf{e} \in \mathbb{R}^{2k}$, $\mathbf{c} \in \mathbb{R}^{2k}$ and $f \in \mathbb{R}$ given by

$$\mathbf{A} = \begin{bmatrix} 0 & \mathbf{I} \\ -\mathbf{\Omega}^2 & -\mathbf{\Gamma} \end{bmatrix}, \qquad \mathbf{e} = \begin{bmatrix} 0 \\ \boldsymbol{\varphi}_{\mathrm{d}} \end{bmatrix},$$
$$\mathbf{c}^{\mathrm{T}} = \left[-\boldsymbol{\varphi}_{\mathrm{y}}^{\mathrm{T}}\mathbf{\Omega}^2\ -\boldsymbol{\varphi}_{\mathrm{y}}^{\mathrm{T}}\mathbf{\Gamma}\right], \quad f = \boldsymbol{\varphi}_{\mathrm{y}}^{\mathrm{T}}\boldsymbol{\varphi}_{\mathrm{d}}. \tag{14}$$

2.2 Test Setup

The test setup for the proposed observer concept is a cantilever steel beam (see Fig. 1) with the parameters given in Table 1 which can be modeled using the approach shown in Sec. 2.1. The beam is fixed at one end and a time varying load is applied on the opposing free end. An acceleration sensor is installed at the free end. The sensor introduces measurement noise with a variance of σ_{acc}^2.

abbreviation	name	value	unit
l	Length	0.3	m
w	Width	0.04	m
h	Height	0.004	m
ρ	Density	8000	kg/m^3
E	Young's modulus	200	GPa
ν	Poisson coefficient	0.305	[–]
σ_{acc}^2	Sensor noise variance	1	(m/s^2)^2

Table 1. Names and values of parameters

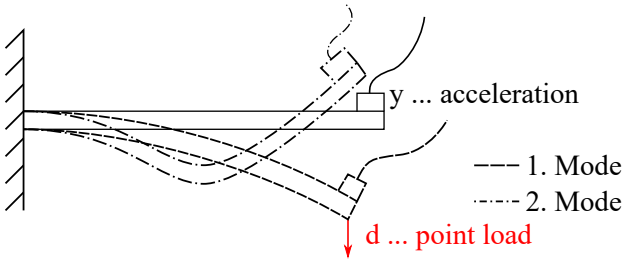

Fig. 1. Cantilever beam with force and acceleration sensor

mode j	1	2	3
$\omega_{0,j}$ in $\frac{\mathrm{rad}}{\mathrm{s}}$	216.8	1344	3843
γ_j in $\frac{1}{\mathrm{s}}$	12.0	13.6	17.0

Table 2. Eigenfrequencies $\omega_{0,j}$ and corresponding modal damping γ_j

For this beam, the eigenmodes are analyzed by use of a finite element simulation tool. The first three eigenmodes of the cantilever beam are considered in the simulation. Their frequencies and damping ratios are given in Table 2. The corresponding eigenvectors depend on the considered location on the beam. For the free end of the beam the eigenvectors are given by $\boldsymbol{\varphi}_{\mathrm{d}}^{\mathrm{T}} = \boldsymbol{\varphi}_{\mathrm{y}}^{\mathrm{T}} = [2.8\ 2\ 1]$. From these parameters a linear system description as given by (13) is constructed. The transfer function from unknown input d to output y is given by

$$G_{\mathrm{yd}}(s) = \sum_{j=1}^{k} \frac{s^2\varphi_{\mathrm{y}j}\varphi_{\mathrm{d}j}}{s^2 + \gamma_j s + \omega_{0,j}^2} = \frac{s^2\nu(s)}{\mu(s)} \tag{15}$$

and its Bode plot is shown in Fig. 2. The resonance frequencies corresponding to the eigenvalues are clearly visible as peaks in the gain plot.

2.3 Observability Analysis

In this section strong observability and strong detectability as introduced by Hautus (1983) are briefly recapitulated and used for analyzing the system (13).

A system is called *strongly observable* if the state vector $\mathbf{x}$ is zero when the output y is zero, for every initial condition $\mathbf{x}_0$ and unknown input d, i.e.

$$y(t) = 0\ \forall\ t \geq 0 \Rightarrow \mathbf{x}(t) = 0\ \forall\ d(t). \tag{16}$$

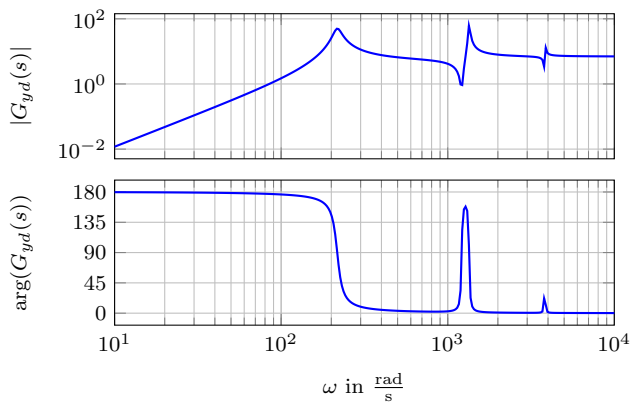

Fig. 2. Transfer function G_{yd} for the cantilever beam

A system is called *strongly detectable* if the state vector $\mathbf{x}$ tends to zero asymptotically when the output y is zero, for every initial condition $\mathbf{x}_0$ and unknown input d, i.e.

$$y(t) = 0 \;\forall\; t \geq 0 \Rightarrow \lim_{t\to\infty} \mathbf{x}(t) = 0 \;\forall\; d(t) \tag{17}$$

Strong observability and strong detectability are connected to the zeros ζ_i of the system. A system is strongly detectable if and only if all zeros ζ_i are located in the left open half plane of $\mathbb{C}$ ($\text{Re}(\zeta_i) < 0$). A system is strongly observable if and only if it has no zeros.

Maes et al. (2015) thoroughly analyzed the observability properties of structural systems, especially for different sensors, and concluded that the exclusive use of acceleration sensors causes stability problems in standard observer design. These stability problems will be briefly discussed by means of the system transfer function (15). The zeros of $G_{\text{yd}}(s)$ can be split up into two groups. All zeros in the first group $\nu(s)$ have negative real part for mechanical systems. The second group consists of two zeros at $\zeta_i = 0$, which stem from the acceleration measurement. Since not all zeros of the transfer function lie in the left open half plane of $\mathbb{C}$, the system is not strongly detectable and a classical UIO for the system will not be stable.

The fact that a mechanical system with only acceleration sensors is not strongly detectable can be seen intuitively if one considers a constant force acting on it. A constant force induces a static displacement in the system, but the output y becomes zero and therefore condition (17) is violated. This means that the acceleration measurement does *not* contain any information about static displacement and the constant part of a force can not be reconstructed.

3. MOTIVATING EXAMPLE

In order to motivate the proposed observer concept, the potential drawbacks of an established method are discussed in the following section. The considered method is an AKF with dummy measurements to circumvent stability issues, as described in Naets et al. (2015). The AKF is given by

$$\begin{aligned} \dot{\hat{\mathbf{x}}}_{\text{e}} &= \mathbf{A}\hat{\mathbf{x}}_{\text{e}} + \mathbf{P}\mathbf{c}\mathbf{R}^{-1}(\mathbf{y}_{\text{e}} - \mathbf{c}^{\text{T}}\hat{\mathbf{x}}_{\text{e}}) \\ \dot{\mathbf{P}} &= -\mathbf{P}\mathbf{c}\mathbf{R}^{-1}\mathbf{c}^{\text{T}}\mathbf{P} + \mathbf{A}\mathbf{P} + \mathbf{P}\mathbf{A}^{\text{T}} + \mathbf{Q} \end{aligned} \tag{18}$$

with initial conditions

$$\hat{\mathbf{x}}_{\text{e}}(t=0) = \mathbf{0} \quad \text{and} \quad \mathbf{P}(t=0) = \mathbf{Q}, \tag{19}$$

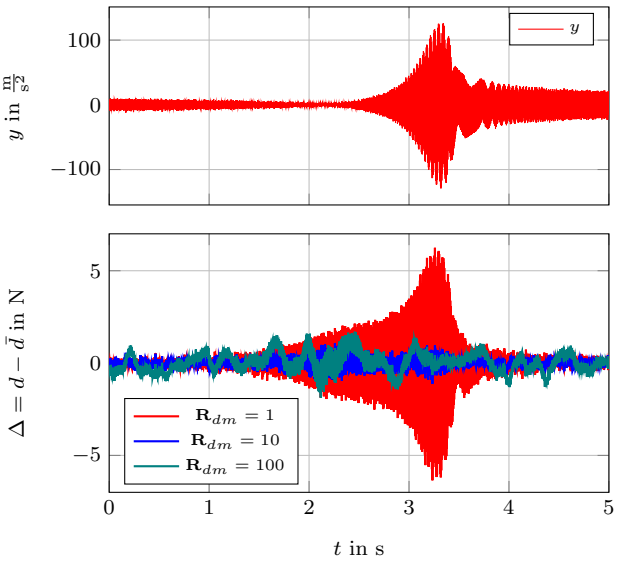

Fig. 3. Measured acceleration y, estimation results $\bar{d}$ and estimation error $\Delta = d - \bar{d}$ of the AKF for a chirp signal as excitation force

where the augmented state vector $\dot{\hat{\mathbf{x}}}_{\text{e}} = \begin{bmatrix}\hat{\mathbf{x}} & \bar{d}\end{bmatrix}^{\text{T}}$ includes the estimate for the unknown input $\bar{d}$. The measurement vector $\mathbf{y}_{\text{e}} = [y \; y_{\text{dm}}]^{\text{T}}$ includes the so-called dummy measurement y_{dm}, which is an artificial position output that is kept at $y_{\text{dm}} = 0$ to avoid a drift of the observer. The covariances for the states and outputs are given by

$$\mathbf{Q} = \begin{bmatrix} 0 & 0 & 0 \\ 0 & Q_{\text{st}} & 0 \\ 0 & 0 & Q_{\text{ui}} \end{bmatrix}, \quad \mathbf{R} = \begin{bmatrix} R_{\text{acc}} & 0 \\ 0 & R_{\text{dm}} \end{bmatrix} \tag{20}$$

with Q_{st}, Q_{ui}, R_{acc} and R_{dm} as the covariance of the states, the augmented state, the acceleration measurements and the dummy measurements, respectively. Q_{st} and R_{acc} are given by the system setup, but Q_{ui} and R_{dm} are design parameters. The AKF is especially sensitive to R_{dm}. In Naets et al. (2015) it is suggested that R_{dm} should be an order of magnitude higher than the systems actual motion.

To illustrate the effects of changing R_{dm}, the AKF is applied to system (13). The system is excited by a chirp signal with linearly increasing frequency (150Hz – 250Hz)

$$d(t) = 2\sin\left(2\pi\left(150t + 10t^2\right)\right), \tag{21}$$

which matches the resonance frequency $\omega_{0,2}$ of the system at $t = 3.25\,\text{s}$. Fig. 3 shows the results of the simulation studies. After analyzing the systems movement for the given disturbance, a variance of $R_{\text{dm}} = 10$ is chosen as suggested in Naets et al. (2015). If the variance is chosen too small ($R_{\text{dm}} = 1$) for the structures' movement a high estimation error occurs near the resonance frequency. If it is chosen too high ($R_{\text{dm}} = 100$) the noise level in the estimation result $\bar{d}$ increases. The determination of R_{dm} can be challenging because the systems actual motion highly depends on the amplitude and frequency of the excitation force d.

4. DESIGN OF A STABILIZED OBSERVER

In this section presents the design of a stable observer that does not assume any prior knowledge of the excitation force d. The general idea of the proposed observer design

is to reconstruct only the dynamic forces acting on the structure and make the observer insensitive with respect to static forces. The observer design includes two steps. First, an standard unknown input observer is designed that reconstructs all dynamic forces but whose estimation dynamics are not stable. And second, the observer is extended with and additional filter to remove the unstable poles and stabilize the estimation dynamics.

4.1 Unknown Input Observer Design

For the observer design, consider a system as in Sec. 2.1

$$\Sigma: \quad \begin{aligned} \dot{\mathbf{x}} &= \mathbf{A}\mathbf{x} + \mathbf{e}d \\ y &= \mathbf{c}^{\mathrm{T}}\mathbf{x} + fd \end{aligned} \tag{22}$$

with matrices defined by (14). Due to the acceleration measurements, system (22) has a direct-feedthrough term $f \neq 0$. Therefore it is possible to calculate the disturbance

$$d = -f^{-1}\mathbf{c}^{\mathrm{T}}\mathbf{x} + f^{-1}y \tag{23}$$

from the system's output through direct inversion. Inserting (23) into the state equation of system (22) gives

$$\dot{\mathbf{x}} = \left(\mathbf{A} - \mathbf{e}f^{-1}\mathbf{c}^{\mathrm{T}}\right)\mathbf{x} + \mathbf{e}f^{-1}y. \tag{24}$$

By introducing new system matrices

$$\begin{aligned} \hat{\mathbf{A}} &= \mathbf{A} - \mathbf{e}f^{-1}\mathbf{c}^{\mathrm{T}}, \quad \hat{\mathbf{e}} = \mathbf{e}f^{-1}, \\ \hat{\mathbf{c}}^{\mathrm{T}} &= -f^{-1}\mathbf{c}^{\mathrm{T}}, \qquad \hat{f} = f^{-1} \end{aligned} \tag{25}$$

the system dynamics can be given as

$$\begin{aligned} \dot{\mathbf{x}} &= \hat{\mathbf{A}}\mathbf{x} + \hat{\mathbf{e}}y \\ d &= \hat{\mathbf{c}}^{\mathrm{T}}\mathbf{x} + \hat{f}y \end{aligned} \tag{26}$$

where all zeros of Σ become eigenvalues of $\hat{\mathbf{A}}$ as described, for example, in Lunze (2017). The system (26) has no measurable output. Therefore, it is only possible to use a trivial observer, which is given by

$$\hat{\Sigma}_{\mathrm{O}}: \quad \begin{aligned} \dot{\hat{\mathbf{x}}} &= \hat{\mathbf{A}}\hat{\mathbf{x}} + \hat{\mathbf{e}}y \\ \hat{d} &= \hat{\mathbf{c}}^{\mathrm{T}}\hat{\mathbf{x}} + \hat{f}y. \end{aligned} \tag{27}$$

All eigenvalues of $\hat{\Sigma}_{\mathrm{O}}$ are determined by the zeros ζ_i of the system Σ. As described in Sec. 2.3 the system Σ has two zeros $\zeta_i = 0$ which result in two eigenvalues $\lambda_0 = 0$ of the observer. These two eigenvalues lead to high amplification of low-frequency components and render the estimation dynamics not asymptotically stable. A solution for this problem is given in the next section.

4.2 Extension for Stabilization

In order to stabilize the observer $\hat{\Sigma}_{\mathrm{O}}$, it is extended with an additional filter

$$\Sigma_{\mathrm{E}}: \quad \begin{aligned} \dot{\mathbf{x}}_{\mathrm{E}} &= \mathbf{A}_{\mathrm{E}}\mathbf{x}_{\mathrm{E}} + \mathbf{b}_{\mathrm{E}}\hat{d} \\ \tilde{d} &= \mathbf{c}_{\mathrm{E}}^{\mathrm{T}}\mathbf{x}_{\mathrm{E}} + d_{\mathrm{E}}\hat{d} \end{aligned} \tag{28}$$

with $\mathbf{x}_{\mathrm{E}} \in \mathbf{R}^2$ and the system matrices

$$\begin{aligned} \mathbf{A}_{\mathrm{E}} &= \begin{bmatrix} -\omega_g & 0 \\ -\omega_g & -\omega_g \end{bmatrix}, \quad \mathbf{b}_{\mathrm{E}} = \begin{bmatrix} \omega_g \\ \omega_g \end{bmatrix}, \\ \mathbf{c}_{\mathrm{E}}^{\mathrm{T}} &= \begin{bmatrix} -1 & -1 \end{bmatrix}, \qquad d_{\mathrm{E}} = 1. \end{aligned} \tag{29}$$

The structure of the filter is chosen such that it has high-pass characteristics (see Fig. 4) and limits the low-frequency amplification of the observer. From the chosen structure it follows that the additional filter has two zeros at the origin of the complex plane. The cut-off frequency ω_g of the filter is the only tuning parameter of the observer.

The systems (26) and (28) can be combined to

$$\tilde{\Sigma}_{\mathrm{O}}: \quad \begin{aligned} \dot{\tilde{\mathbf{x}}} &= \tilde{\mathbf{A}}\tilde{\mathbf{x}} + \tilde{\mathbf{e}}y \\ \tilde{d} &= \tilde{\mathbf{c}}^{\mathrm{T}}\tilde{\mathbf{x}} + \tilde{f}y \end{aligned} \tag{30}$$

with system matrices

$$\begin{aligned} \tilde{\mathbf{A}} &= \begin{bmatrix} \hat{\mathbf{A}} & \mathbf{0} \\ \mathbf{b}_{\mathrm{E}}\hat{\mathbf{c}}^{\mathrm{T}} & \mathbf{A}_{\mathrm{E}} \end{bmatrix}, \quad \tilde{\mathbf{e}} = \begin{bmatrix} \hat{\mathbf{e}} \\ \mathbf{b}_{\mathrm{E}}\hat{f} \end{bmatrix}, \\ \tilde{\mathbf{c}}^{\mathrm{T}} &= \begin{bmatrix} d_{\mathrm{E}}\hat{\mathbf{c}}^{\mathrm{T}} & \mathbf{c}_{\mathrm{E}}^{\mathrm{T}} \end{bmatrix}, \qquad \tilde{f} = d_{\mathrm{E}}\hat{f} \end{aligned} \tag{31}$$

and the state vector $\tilde{\mathbf{x}} = \begin{bmatrix} \hat{\mathbf{x}} & \mathbf{x}_{\mathrm{E}} \end{bmatrix}^{\mathrm{T}}, \tilde{\mathbf{x}} \in \mathbf{R}^{2k+2}$. The system $\tilde{\Sigma}_{\mathrm{O}}$ also includes the two unstable eigenvalues $\lambda_0 = 0$. The eigenvalues at λ_0 are not observable due to the zeros of the additional filter as shown in Appendix A.

It is possible to find a Kalman decomposition of $\tilde{\Sigma}_{\mathrm{O}}$

$$\begin{aligned} \bar{\mathbf{A}} &= \mathbf{T}\tilde{\mathbf{A}}\mathbf{T}^{\mathrm{T}} = \begin{bmatrix} \tilde{\mathbf{A}}_{\bar{\mathrm{O}}} & \tilde{\mathbf{A}}_{12} \\ \mathbf{0} & \tilde{\mathbf{A}}_{\mathrm{O}} \end{bmatrix}, \quad \bar{\mathbf{e}} = \mathbf{T}\tilde{\mathbf{e}} = \begin{bmatrix} \tilde{\mathbf{e}}_{\bar{\mathrm{O}}} \\ \tilde{\mathbf{e}}_{\mathrm{O}} \end{bmatrix}, \\ \bar{\mathbf{c}}^{\mathrm{T}} &= \tilde{\mathbf{c}}^{\mathrm{T}}\mathbf{T}^{\mathrm{T}} = \begin{bmatrix} \mathbf{0}^{\mathrm{T}} & \tilde{\mathbf{c}}_{\mathrm{O}}^{\mathrm{T}} \end{bmatrix}, \qquad \bar{f} = \tilde{f}. \end{aligned} \tag{32}$$

as described in Kalman (1963) using a similarity transformation matrix $\mathbf{T}$. The matrix $\mathbf{T}$ can be determined, for example, via the method proposed in Boley (1984). The resulting dynamic matrix $\bar{\mathbf{A}} \in \mathbb{R}^{2k+2\times 2k+2}$ has two parts, a fully observable part $\tilde{\mathbf{A}}_{\mathrm{O}} \in \mathbb{R}^{2k\times 2k}$ and an unobservable part $\tilde{\mathbf{A}}_{\bar{\mathrm{O}}} \in \mathbb{R}^{2\times 2}$. The unobservable part $\tilde{\mathbf{A}}_{\bar{\mathrm{O}}}$ consists of the two unstable eigenvalues λ_0. $\tilde{\mathbf{A}}_{\bar{\mathrm{O}}}$ does not influence the output $\tilde{d}$ and can be excluded from the implementation of the observer. The final observer is given by

$$\bar{\Sigma}_{\mathrm{O}}: \quad \begin{aligned} \dot{\bar{\mathbf{x}}} &= \tilde{\mathbf{A}}_{\mathrm{O}}\bar{\mathbf{x}} + \tilde{\mathbf{e}}_{\mathrm{O}}y \\ \bar{d} &= \tilde{\mathbf{c}}_{\mathrm{O}}^{\mathrm{T}}\bar{\mathbf{x}} + \tilde{f}y \end{aligned} \tag{33}$$

with $\bar{\mathbf{x}} \in \mathbf{R}^{2k}$. The observer $\bar{\Sigma}_{\mathrm{O}}$ does not include the unstable eigenvalues λ_0 and can reconstruct the dynamic forces acting on the structure.

5. OBSERVER TUNING

This section discusses the influence of the only design parameter ω_g on the observer performance and gives guidelines on how to choose this parameter. The value of ω_g has two different effects on the observer performance. First, it introduces an amplitude and phase error for low frequency components and second, it influences the noise amplification of the observer. These effects can be shown using the transfer functions $\bar{G}_O(s)$ and $G_E(s)$ corresponding to the observer $\bar{\Sigma}_{\mathrm{O}}$ and additional filter Σ_{E}, respectively.

5.1 Amplitude and Phase Error for Low Frequencies

For a perfect reconstruction of the unknown input the relation

$$G_{\bar{\mathrm{d}}\mathrm{d}}(s) = \frac{\bar{d}(s)}{d(s)} = 1 \tag{34}$$

should hold for the transfer function of the dynamic behavior from the unknown input d to the estimation of the observer $\bar{d}$. The overall transfer function $G_{\bar{\mathrm{d}}\mathrm{d}}(s)$ for system Σ and observer $\bar{\Sigma}_{\mathrm{O}}$ is equal to $G_E(s)$. The transfer function $G_E(s)$ violates condition (34) for low frequencies

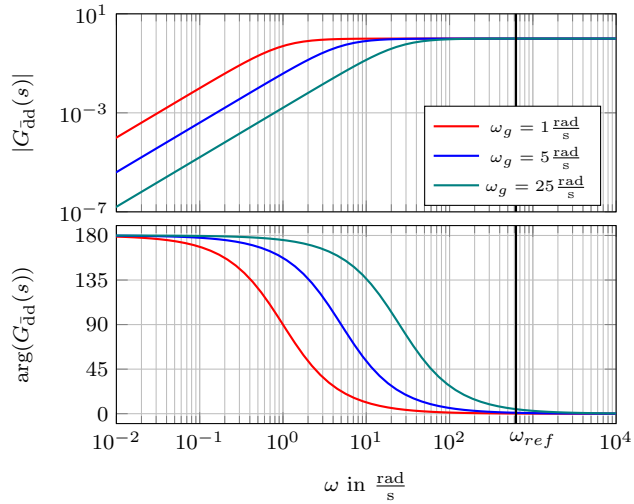

Fig. 4. Transfer function from input to estimation of unknown input $G_{\bar{\mathrm{dd}}}(s) = G_E(s)$

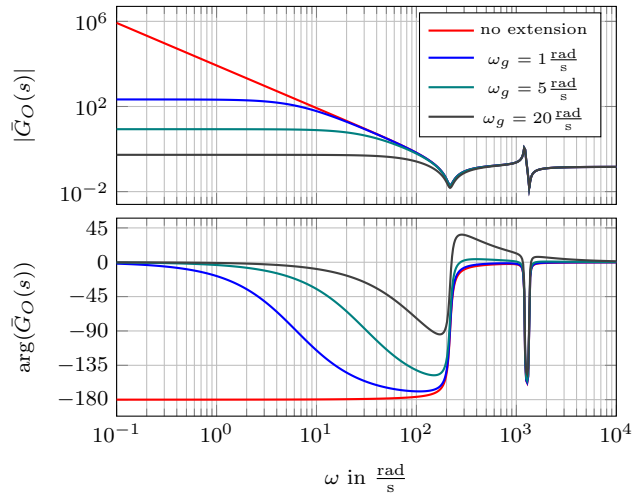

Fig. 5. Observer transfer function $\bar{G}_O(s)$ for different ω_g

as can be seen in Fig. 4. An amplitude and phase error is introduced and can be defined as

$$\Delta A = |G_E(j\omega_{ref})| \tag{35}$$
$$\Delta\varphi = \arg(G_E(j\omega_{ref})) \tag{36}$$

at a frequency ω_{ref}, defined by the applications frequency range of interest. In Fig. 6 the phase error $\Delta\varphi$ is depicted as function of ω_g. It increases linearly with increasing ω_g.

5.2 Noise Gain

The noise gain n_n for band-limited white noise of a system is the ratio of output to input noise within a frequency range $\omega \in [0, \omega_{max}]$. For the observer it describes how the measurement noise is amplified in the estimation of the unknown input. The noise gain n_n can be calculated by

$$n_n = \frac{\sigma_{out}^2}{\sigma_{in}^2} = \frac{1}{2\pi}\int_0^{\omega_{max}} |\bar{G}_O(j\omega)|^2 d\omega \tag{37}$$

where σ_{out}^2 and σ_{in}^2 are the variances of the output and input signal. Fig. 5 depicts the observer transfer function $\bar{G}_O$ for different values of ω_g. Lower values for ω_g result in a higher amplification in the low frequency range. This higher amplification causes a higher noise gain and n_n increases for low values of ω_g, as can be seen in Fig. 6.

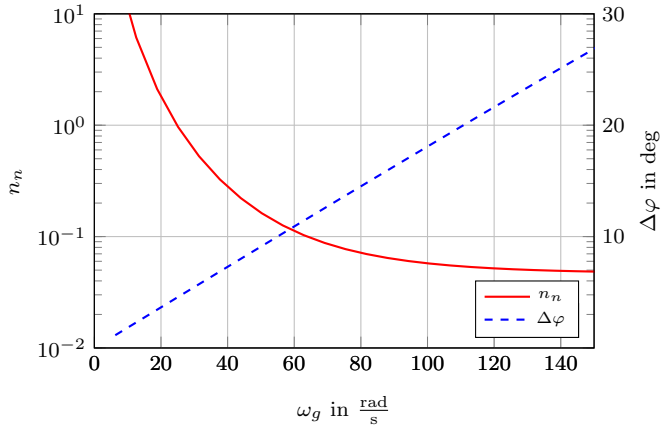

Fig. 6. Phase error $\Delta\varphi$ at $\omega_{ref} = 2 \cdot \pi \cdot 100\frac{\mathrm{rad}}{\mathrm{s}}$ and noise gain n_n over ω_g

5.3 Trade-Off Guidelines

Fig. 6 shows the introduced phase error $\Delta\varphi$ at ω_{ref} and noise gain n_n. For increasing ω_g the phase error $\Delta\varphi$ linearly increases while the noise gain n_n decreases first and approaches a constant value. Therefore two opposing objectives for the tuning parameter ω_g arise:

- choose ω_g as small as possible to minimize the amplitude and phase error
- choose ω_g as big as possible to minimize the noise gain n_n

An appropriate ω_g can be chosen based on a given maximum noise gain $n_{n,max}$, a maximum phase error $\Delta\varphi_{max}$, or by normalizing and weighting both parameters according to requirements.

6. SIMULATION RESULTS

In order to evaluate the applicability and performance of the proposed observer concept (33), it is tested in simulation. The observer is designed for the cantilever beam introduced in Sec. 2.2, using the method proposed in Sec. 4. The observer design parameter is chosen as $\omega_g = 10 \cdot 2 \cdot \pi\,\frac{\mathrm{rad}}{\mathrm{s}}$ following the discussion given in Sec. 5.

To compare the proposed observer concept with a state-of-the-art concept an AKF as proposed in Naets et al. (2015) is implemented. For the variance of the dummy measurement the appropriate value of $R_{\mathrm{dm}} = 10$ is chosen as already discussed in Sec. 3. The variance of the acceleration measurement is assumed to be known with $R_{\mathrm{acc}} = \sigma_{acc}^2$. No model errors are considered therefore the state variance is chosen as $Q_{\mathrm{st}} = 0$. The variance of the augmented state should be considerably higher than the maximum rate of change and is chosen as $Q_{\mathrm{ui}} = 10^5$.

In a first simulation, the acting force is a triangle signal with a frequency of $f = 200\,\mathrm{Hz}$ which starts at $t = 0.01\,\mathrm{s}$. Fig. 7 shows the estimated disturbance and the estimation error $\Delta = d - \bar{d}$. Both concepts are able to give a reasonable estimate of the disturbance with an error within the same range. The estimation error of the AKF is smaller first and increases to a steady magnitude afterwards.

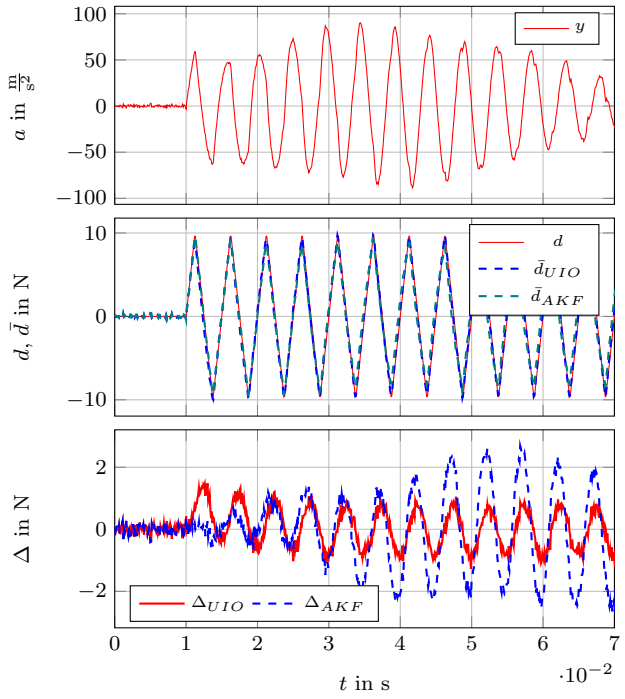

Fig. 7. Simulation: Measured acceleration y, measured disturbance d, estimated disturbances $\bar{d}$, and estimation errors $\Delta = d - \bar{d}$ for a triangle disturbance

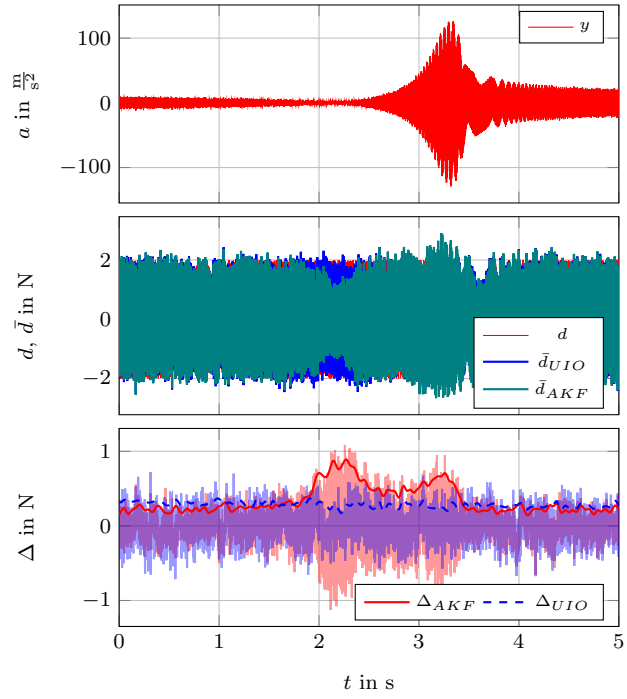

Fig. 8. Simulation: Acceleration y, measured disturbance d, estimated disturbances $\bar{d}$, and estimation errors $\Delta = d - \bar{d}$ for a chirp disturbance

In a second simulation, the acting force is a sine chirp signal defined by (21) to test the observer performance over a frequency range that also includes the resonance frequency $\omega_{0,2}$. The chirp signal starts at $t = 0\,\mathrm{s}$ with a frequency of $f = 150\,\mathrm{Hz}$ and ends at $t = 5\,\mathrm{s}$ with a frequency of $f = 250\,\mathrm{Hz}$. The results of the simulation can be seen in Fig. 8. The estimation error of the UIO stays constant within the frequency range while the estimation error of

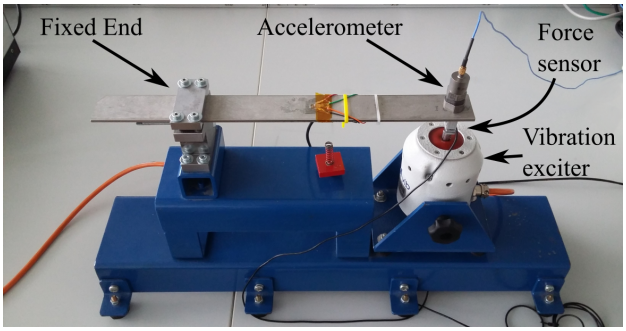

Fig. 9. Experimental setup of the cantilever beam

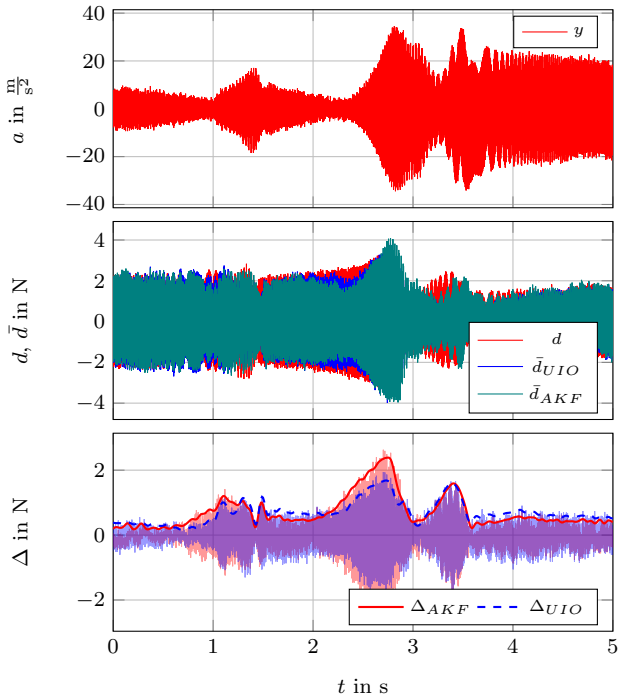

Fig. 10. Experimental Validation: Acceleration y, measured disturbance d, estimated disturbances $\bar{d}$ and estimation error $\Delta = d - \bar{d}$

the AKF increases significantly around $t = 3\,\mathrm{s}$ where the disturbance frequency matches $\omega_{0,2}$. This resonance causes significant system motion, close to the values chosen for R_{dm}, degrading the AKF performance as shown in Sec. 3.

7. EXPERIMENTAL RESULTS

For the experimental validation of the proposed observer a cantilever beam as described in Sec. 2.2 was used and the test setup can be seen in Fig. 9. One end of the beam is fixed and a vibration exciter is attached to the free end with a force sensor in between to measure the applied force. An acceleration sensor is placed on the free end above the force sensor. The system parameters are determined by test measurements and used to find a linear system model of the form of Eq. (14).

The same chirp signal as in the simulation studies in Sec. 6 defined by (21) is used as excitation force of the beam. The chirp signal starts at $t = 0\,\mathrm{s}$ with a frequency of $f = 150\,\mathrm{Hz}$ and ends at $t = 5\,\mathrm{s}$ with a frequency of $f = 250\,\mathrm{Hz}$. The acceleration is measured with a sampling frequency

of $f_s = 10\,\text{kHz}$ and the estimation results and estimation errors for both observer concepts are given in Fig. 10.

Both observer concepts can reconstruct the amplitude of the unknown input, but introduce a phase error higher than expected in observer design and simulation studies. This additional phase error stems from the model error introduced by the linear system approximation. Furthermore it renders the estimation error of the UIO to be not constant in amplitude, contrary to the simulation results. The AKF estimation error is smaller for low frequencies but increases if a resonance frequency is excited, as already shown in the simulation studies in Sec. 6.

8. CONCLUSION AND OUTLOOK

This paper presents an unknwon input observer (UIO) for the estimation of dynamic external forces acting on a mechanical system with only acceleration sensors. The main idea is to extend a classical unknown input observer with an additional filter for stabilization.

It is shown in simulation and experiment that the resulting UIO outperforms the augmented Kalman filter (AKF) if the excitation force frequency matches a resonance frequency of the system. In addition, there are several advantages in the design process of the UIO. First, the UIO has only one tuning parameter ω_g which makes it more appealing to users with little experience in the field of control engineering. Second, in the design process for the UIO no knowledge about the amplitude or frequency of the acting force is necessary. For the AKF this information is required for the tuning of the variance for the augmented state and dummy measurements. And third, the UIO uses a deterministic model while for the design of the AKF the variances for measurements and states should be known as accurately as possible.

In contrast to the AKF approach, the UIO was only tested for SISO systems so far. An extension of the UIO to MIMO systems should be studied further. The proposed observer concept can be used in a wide range of applications like fault detection, structural analysis and system health monitoring, especially if no knowledge about the magnitude of the excitation force is available. The UIO provides better estimation results for an external force than the AKF and needs less system knowledge for tuning.

REFERENCES

Boley, D. (1984). Computing the Kalman decomposition: An optimal method. *IEEE Transactions on Automatic Control*, 29(1), 51–53.

Caughey, T.K. (1960). Classical Normal Modes in Damped Linear Dynamic Systems. *Journal of Applied Mechanics*, 27(2), 269.

Eftekhar Azam, S., Chatzi, E., and Papadimitriou, C. (2015). A dual Kalman filter approach for state estimation via output-only acceleration measurements. *Mechanical Systems and Signal Processing*, 60, 866–886.

Hautus, M.L.J. (1983). Strong Detectability and Observers. *Science*, 368.

Kalman, R.E. (1963). Mathematical Description of Linear Dynamical Systems. *Journal of the Society for Industrial and Applied Mathematics Series A Control*, 1(2), 152–192.

Klinkov, M. (2011). Identification of Unknown Structural Loads from Dynamic Measurements Using Robust Observers. *Doctoral dissertation*.

Lourens, E., Papadimitriou, C., Gillijns, S., Reynders, E., De Roeck, G., and Lombaert, G. (2012). Joint input-response estimation for structural systems based on reduced-order models and vibration data from a limited number of sensors. *Mechanical Systems and Signal Processing*, 29, 310–327.

Lunze, J. (2017). Zustandsbeobachtung linearer Systeme mit unbekannten Eingängen. *at - Automatisierungstechnik*, 65(2), 99–114.

Maes, K., Lourens, E., Van Nimmen, K., Reynders, E., De Roeck, G., and Lombaert, G. (2015). Design of sensor networks for instantaneous inversion of modally reduced order models in structural dynamics. *Mechanical Systems and Signal Processing*, 52-53(1), 628–644.

Naets, F., Cuadrado, J., and Desmet, W. (2015). Stable force identification in structural dynamics using Kalman filtering and dummy-measurements. *Mechanical Systems and Signal Processing*, 50-51, 235–248.

Sanchez, J. and Benaroya, H. (2014). Review of force reconstruction techniques. *Journal of Sound and Vibration*, 333(14), 2999–3018.

Appendix A. OBSERVABILITY ANALYSIS FOR EIGENVALUE λ_0

The Hautus test is used for observability analysis of the eigenvalue λ_0. It states that for an observable system there exists no eigenvector orthogonal to the output matrix $\tilde{\mathbf{c}}^\mathrm{T}$. The corresponding eigenvector $\mathbf{v}_0$ to eigenvalue λ_0 can be calculated by

$$(\tilde{\mathbf{A}} - \lambda_0 \mathbf{I})\mathbf{v}_0 = 0. \tag{A.1}$$

All known parameters can be inserted in (A.1) and the vector $\mathbf{v}_0$ is split into four parts resulting in

$$\begin{bmatrix} \mathbf{0} & \mathbf{I} & \mathbf{0} & \mathbf{0} \\ \mathbf{P}_1\boldsymbol{\Omega}_0 & \mathbf{P}_1\boldsymbol{\Gamma} & \mathbf{0} & \mathbf{0} \\ -\omega_g\mathbf{P}_2\boldsymbol{\Omega}_0 & -\omega_g\mathbf{P}_2\boldsymbol{\Gamma} & -\omega_g & 0 \\ -\omega_g\mathbf{P}_2\boldsymbol{\Omega}_0 & -\omega_g\mathbf{P}_2\boldsymbol{\Gamma} & -\omega_g & -\omega_g \end{bmatrix} \begin{bmatrix} \mathbf{v}_1 \\ \mathbf{v}_2 \\ v_3 \\ v_4 \end{bmatrix} = \mathbf{0} \tag{A.2}$$

with $\mathbf{P}_1 = (\boldsymbol{\varphi}_\mathrm{d}(\boldsymbol{\varphi}_\mathrm{y}^\mathrm{T}\boldsymbol{\varphi}_\mathrm{d})^{-1}\boldsymbol{\varphi}_\mathrm{y}^\mathrm{T} - \mathbf{I})$ and $\mathbf{P}_2 = \boldsymbol{\varphi}_\mathrm{y}^\mathrm{T}(\boldsymbol{\varphi}_\mathrm{y}^\mathrm{T}\boldsymbol{\varphi}_\mathrm{d})^{-1}$. From (A.2) it is possible to calculate the eigenvector $\mathbf{v}_0$ as

$$\mathbf{v}_0 = \begin{bmatrix} \mathbf{q}^\mathrm{T} & \mathbf{0}^\mathrm{T} & -\mathbf{P}_2\boldsymbol{\Omega}_0\mathbf{q} & 0 \end{bmatrix}^\mathrm{T} \tag{A.3}$$

where $\mathbf{q}$ is an eigenvector of $\mathbf{P}_1\boldsymbol{\Omega}_0$ for the eigenvalue zero.

The algebraic multiplicity of λ_0 is two but its geometric multiplicity is one resulting in one linearly independent eigenvector $\mathbf{v}_0$. Therefore it is necessary to find the generalized eigenvector $\mathbf{r}_0$ that can be calculated by

$$(\tilde{\mathbf{A}} - \lambda_0 \mathbf{I})\mathbf{r}_0 = \mathbf{v}_0. \tag{A.4}$$

Similar to the calculation of $\mathbf{v}_0$ all parameters are inserted into (A.4) and the generalized eigenvector is given by

$$\mathbf{r}_0 = \begin{bmatrix} -(\boldsymbol{\Omega}_0^{-1}\boldsymbol{\Gamma}\mathbf{q})^\mathrm{T} & \mathbf{q}^\mathrm{T} & \omega_g^{-1}\mathbf{P}_2\boldsymbol{\Omega}_0\mathbf{q} & -\omega_g^{-1}\mathbf{P}_2\boldsymbol{\Omega}_0\mathbf{q} \end{bmatrix}^\mathrm{T}. \tag{A.5}$$

The product of output matrix

$$\tilde{\mathbf{c}}^\mathrm{T} = [-\mathbf{P}_2\boldsymbol{\Omega}_0 \ -\mathbf{P}_2\boldsymbol{\Gamma} \ -1 \ -1] \tag{A.6}$$

and vectors $\mathbf{v}_0$ and $\mathbf{r}_0$

$$\tilde{\mathbf{c}}^\mathrm{T}\mathbf{v}_0 = 0 \qquad \tilde{\mathbf{c}}^\mathrm{T}\mathbf{r}_0 = 0 \tag{A.7}$$

is always zero, proving that λ_0 is an unobservable eigenvalue of the system $\tilde{\Sigma}_\mathrm{O}$.